ChemComm

Chemical reduction of π-expanded functionalized pentacene: Cooperation of side group in alkali metal binding

Journal:	*ChemComm*
Manuscript ID	CC-COM-07-2024-003318.R2
Article Type:	Communication

COMMUNICATION

Chemical reduction of π-expanded functionalized pentacene: Cooperation of side group in alkali metal binding

Received 00th January 20xx,
Accepted 00th January 20xx

DOI: 10.1039/x0xx00000x

Matthew Pennachio,[a] Zheng Wei,[a] Masashi Mamada,[b] Michel Frigoli[c*] and Marina A. Petrukhina[a*]

Chemical reduction of a vertically expanded pentacene, TIPS-*peri*-pentacenopentacene (TIPS-PPP), with sodium metal in THF readily afforded a doubly-reduced product isolated as [{Na$^+$(THF)$_3$}$_2$(TIPS-PPP^{2-})]. Single-crystal X-ray diffraction revealed the formation of a π-complex of TIPS-PPP^{2-} with two {Na$^+$(THF)$_3$} moieties. The sodium ion is coordinated to three C-atoms at the most negatively charged edge sites and at the lateral ethynyl group. The delocalisation of the charge on the ethynyl function is accompanied by its notable elongation (Δ = 0.015 Å) coupled with the contraction of the adjacent single C–C bond (Δ = 0.033 Å). Bond length analysis supported by Harmonic Aromaticity Oscillator Model (HOMA) shows that the dianion can be written with four aromatic sextets in agreement with the Clar representation. Although TIPS-PPP^{2-} has 36 π-electrons (4n), it does not show a global magnetic paratropic response. The rings with the most negative charge density have a very low paratropic response, while the other rings have a low diatropic response. Overall, the dianion is a non-aromatic molecule.

Linear acenes, composed of laterally fused benzene rings, have attracted significant interest from fundamental and applied viewpoints.[1,2] While these organic materials have been studied for well over a century, their use in optoelectronic applications such as organic light emitting diodes (OLEDs), photovoltaic devices (OPVs), and organic field-effect transistors (OTFTs) has generated a resurgence of interest in recent decades.[3–9] Pentacene and its derivatives are regarded as representatives of the most active small-molecule semiconductor materials for organic thin-film transistors due to their high charge carrier mobility, low-lying triplet states, low ionization potentials, small optical gaps, and high electron affinities. Furthermore, the singlet fission (SF) effect, which produces more than one charge-carrier per one absorbed photon, may yield photovoltaic efficiencies up to 200 %.[10–13]

However, despite these advances, investigation into neat longer acenes is fraught with stability, reactivity, and solubility issues.[14]

The seminal work by Anthony *et al.*[15,16] reported the preparation of a pentacene functionalized with two triisopropylsilylethynyl groups (TIPS, denoted as **TIPS-pen**, Figure 1) that lead to an efficient face-to-face π-π stacking in the solid-state, yielding good semiconducting properties. As a conceptual vertical expansion, TIPS-*peri*-pentacenopentacene (**TIPS-PPP**, $C_{56}H_{56}Si_2$) was synthesized recently as a π-expanded functionalized pentacene.[17] **TIPS-PPP** behaves as a p-type semiconductor and has enabled a six-fold increase in charge mobility in OFET devices compared to **TIPS-pen**.[18]

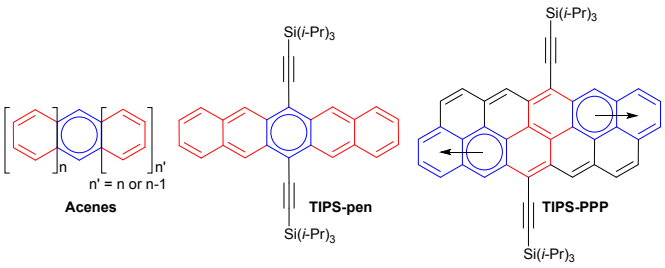

Fig. 1 General depiction of acenes, **TIPS-pen**, and **TIPS-PPP**.

In our recent work, we have shown that the parent pentacene serves as a two-electron acceptor in chemical reduction reactions with all Group 1 metals.[19] Specifically, the Group 1 congeners all form π-complexes in which the alkali metal is coordinated to the central six-membered ring, consistent with computational and ^{1}H NMR spectroscopic investigations demonstrating that the negative charge is concentrated on the central acene ring. In addition, one solvent-separated ion product was isolated with the help of benzo-15-crown-5 ether enabling the formation of the 'naked' pentacene dianion. In this work, we aimed to investigate the chemical reduction behavior of the π-expanded and

[a] *Department of Chemistry, University at Albany, State University of New York, Albany, NY 12222, USA*
[b] *Department of Chemistry, Graduate School of Science, Kyoto University, Sakyo-ku, Kyoto 606-8502, Japan*
[c] *UMR CNRS 8180, UVSQ, Institut Lavoisier de Versailles, Université Paris-Saclay, 45 Avenue des Etats-Unis, 78035 Versailles Cedex, France*
Electronic Supplementary Information (ESI) available: Details of preparation, X-ray diffraction and computational study. CCDC 2367428. For ESI and crystallographic data in CIF or other electronic format see DOI: xxxxxxxxxxxxx

functionalized pentacene derivative, **TIPS-PPP**. We revealed that it readily accepts two electrons in the Na-induced reduction reaction. The resulting product was isolated and fully characterized by X-ray crystallography, UV-Vis and NMR spectroscopy. The change in tropicity upon double reduction is also highlighted by theoretical calculations such as nucleus-independent chemical shifts (NICS) and anisotropy of the induced current density (ACID) plot.[20]

The chemical reduction of **TIPS-PPP** with Na metal was investigated in THF at room temperature and monitored by UV-Vis absorption spectroscopy (Fig. S1). The first reaction step is accompanied by the appearance of a light brown color, which quickly changes to a dark brown color, indicating the formation of a doubly-reduced product in solution. Through slow diffusion of hexanes into the THF solution, dark brown needles deposited in moderate yield. Single-crystal X-ray diffraction analysis confirmed the formation of a π-complex, namely [{$Na^+(THF)_3$}$_2$(**TIPS-PPP^{2-}**)] (Scheme 1), abbreviated **Na_2-TIPS-PPP^{2-}**.

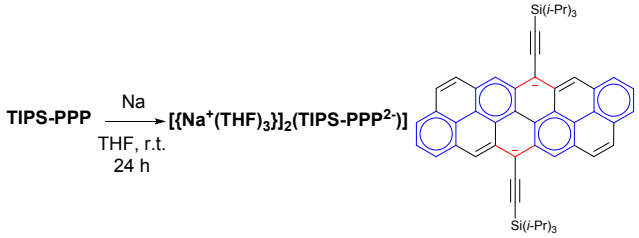

Scheme 1 Chemical reduction of **TIPS-PPP** with sodium metal and Clar structure of **TIPS-PPP^{2-}**.

Na_2-TIPS-PPP^{2-} crystallizes in centrosymmetric triclinic space group *P*-1 with Z = 1. In the crystal structure, there are two crystallographically equivalent Na^+ ions coordinated to one **TIPS-PPP^{2-}** dianion with Na–C distances spanning over 2.6342(7)–2.8254(6) Å) range (Fig. 2). More specifically, Na^+ ions are coordinated to three carbon atoms on the edge and to the adjacent acetylenic carbon of the TIPS functional group. Each Na^+ ion is also capped by three THF molecules with the Na···O_{THF} bond distances ranging from 2.2340(7) to 2.2531(6) Å (Fig. 2). All Na–C and Na–O distances are comparable to those previously reported.[21,22] In the solid-state structure (Fig. 3),

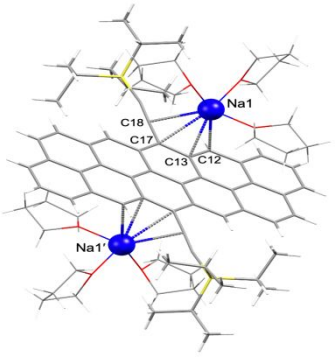

Bond	Distance(Å)
Na–C12	2.7501(7)
Na–C13	2.6342(7)
Na–C17	2.7100(6)
Na–C18	2.8254(6)

Fig. 2 Crystal structure of **Na_2-TIPS-PPP^{2-}**, along with the Na–C distances.

extended 1D columns are formed by strong C–H···π interactions between the **TIPS-PPP^{2-}** anions and the cationic {$Na^+(THF)_3$} moieties measured at 2.284(4) Å (Fig. S8).

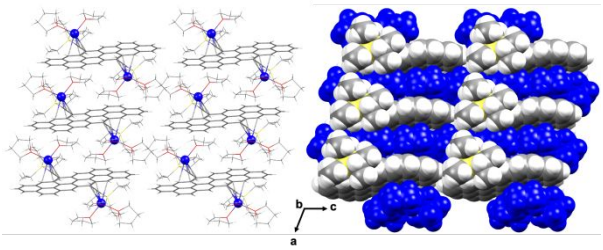

Fig. 3 Solid-state packing of **Na_2-TIPS-PPP^{2-}**, ball-and-stick and space-filling models.

Importantly, the ethynyl groups that participate in the coordination of the {$Na^+(THF)_3$} cations are affected by the reduction and by the delocalization of the negative charges (Fig. 4). Specifically, the acetylenic bond is elongated to 1.2217(8) Å in **TIPS-PPP^{2-}** versus 1.207(5) Å in **TIPS-PPP**, while the adjacent bond is notably contracted to 1.4039(7) in **TIPS-PPP^{2-}** versus 1.438(4) Å in **TIPS-PPP**. While the polyaromatic core of **TIPS-PPP** remains almost planar after the acquisition of two electrons, the bond length alternations (BLAs) at the periphery are significantly modified between the neutral form and the doubly-reduced form (Fig. 4).

It should be noted that, although the aromatic sextet was initially positioned only on the B rings for the neutral form,[17] the BLAs around the A rings average around 0.045 Å, which is similar to the BLAs observed for naphthalene (see ESI). Although the HOMA value of the A rings is lower than that of a naphthalene

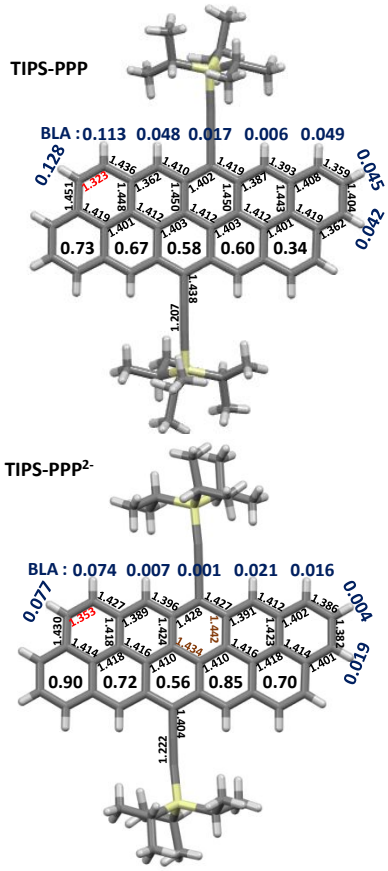

Fig. 4 Crystal bond lengths of **TIPS-PPP** (top) and **TIPS-PPP^{2-}** (bottom) generated with Mercury software (https://www.ccdc.cam.ac.uk/solutions/software/free-mercury/), as well as bond length alternation (BLA) and HOMA values inside the rings. See Table S3 for more details.

due to a long bond length between the A and B rings, it is likely that the aromatic sextet is distributed between the A and B rings, as shown in Fig. 1.

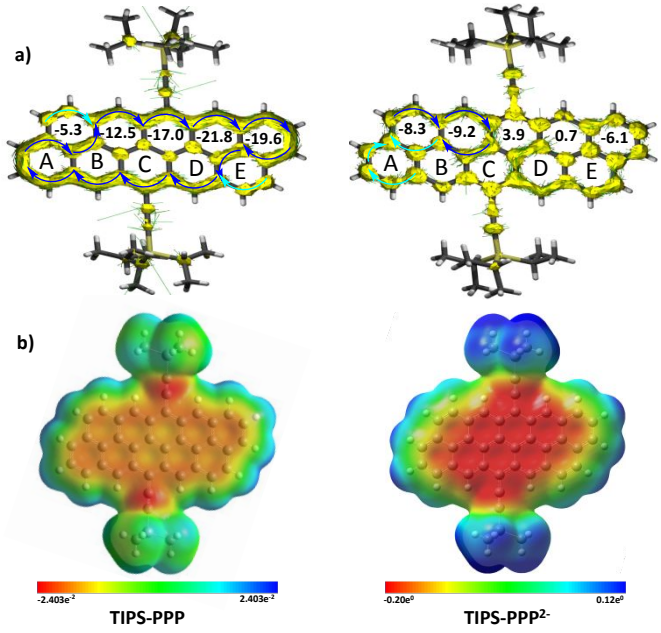

Fig. 5 a) π-only ACID plots with NICS (1.7)$_{\pi zz}$ values based on crystal structures; b) Molecular electrostatic potential maps (Blue: positive and red: negative) of **TIPS-PPP** (left) and **TIPS-PPP^{2-}** (right).

In contrast of the neutral **TIPS-PPP**, its reduced form contains four aromatic sextets on A and D rings according to the Clar structure of **TIPS-PPP^{2-}** (Scheme 1). The two-fold reduction of **TIPS-PPP** generates two pyrene moieties with negative charge concentrated on C rings that can easily be delocalized on B rings and on the ethynyl groups without altering the aromatic sextets. The molecular electrostatic potential map (MEP, Fig. 5b) of **TIPS-PPP^{2-}** is consistent with these assumptions. To a much lesser extent, the delocalization of the negative charge occurs partially on the D rings.

According to the MEP, the location of sodium ions is controlled by the charge density of the carbon sites. The presence of the TIPS-ethynyl fragment probably plays a central role in sodium ion coordination, not only through its own charge density, but also by controlling steric hindrance around the center of the molecule and therefore the packing. Thus, the study of the reduction of **TIPS-Pen** is interesting in this regard and may give valuable information about the role of the presence of TIPS-ethynyl groups.

The crystal structure of **TIPS-PPP^{2-}** fits very well with the Clar representation regarding the bong lengths. Bond length analysis for the backbone of **TIPS-PPP^{2-}** reveals that E rings have the shortest bond length (bond marked in red) of 1.353 Å that is as short as that of the typical localized double bond observed in the outer rings of acenes or in the center rings of pyrene molecule.[17] The center C rings that holds the largest negative charge have the longest bond lengths at the periphery, around 1.427 Å with the longest bond lengths on the inside (bonds marked in brown, Figure 4 bottom). The D rings have a BLA as small as 0.007 Å, suggesting an aromatic sextet. The B rings have a BLA of 0.021 Å, observed in a similar way in the second and fourth rings of the doubly-reduced pentacene for which the BLA values vary from 0.014 to 0.021 Å depending on the nature of the metal used and the reliability factor.[19] Finally, the A rings have a BLA of 0.016 Å at the periphery and a BLA of 0.004 Å on the edge suggesting an aromatic sextet.

Analysis of the Harmonic Aromaticity Oscillator Model (HOMA)[23] agrees with the bond length analysis at the periphery and edge and shows that in **TIPS-PPP^{2-}** the highest values are observed for A (0.90) and D (0.85) rings, which is consistent with the fact that these are the aromatic sextets (Scheme 1). It should be noted that a HOMA value of 0.90 corresponds to the value obtained for the aromatic sextets in pyrene (see ESI). The lowest HOMA value is observed for C rings (0.56) followed by rings E (0.70) and B (0.72).

Although **TIPS-PPP^{2-}** can be written with 4 aromatic sextets, it has 4n (36) π-electrons like any antiaromatic system. However, under magnetic field, it does not show a global magnetic paratropic response as observed during the two-fold reduction of pentacene, even though the dianion of pentacene can be written with two aromatic sextets on the outer rings.[19] On the contrary, the ACID plot of **TIPS-PPP^{2-}** shows that a weak clockwise diatropic ring current is located on D and E rings and very weak one on A rings (Fig. 5a). Consequently, the negative NICS values on these rings are low. Only rings B and C, which have the highest density of negative charges, have very low positive NICS values and no counter-clockwise paratropic current is observed in the ACID plot. As a result, based on the magnetic response, the dianion can be considered as a non-aromatic molecule overall.

Notably, the doubly-reduced form **TIPS-PPP^{2-}** behaves differently under a magnetic field than the doubly-oxidized form **TIPS-PPP^{2+}** for which all the rings retain a diatropic ring current but with a much lower intensity than for **TIPS-PPP**.[24] Given that the Clar structures of the two ionic species are the same and that the delocalization of negative or positive charges is very similar according to the MEP maps (see ESI), the difference in tropicity of the two charged species comes from the orbitals that contribute significantly to the ring current, for which usually HOMO and LUMO contribute the most.[25,26] As the shape of the HOMO and LUMO of the two species are different, their tropicity is different. It is interesting to note that the HOMO of **TIPS-PPP^{2-}** is similar to the LUMO of **TIPS-PPP** and the LUMO of **TIPS-PPP^{2+}** is similar to the HOMO of **TIPS-PPP** (see ESI).

The doubly-reduced **TIPS-PPP^{2-}** anion is stable in THF solution in the absence of moisture and air and exhibits characteristic signals in the ^{1}H NMR spectrum at −80 °C (Fig. 6). The addition of two electrons to **TIPS-PPP** is accompanied by strong upfield shifts of the protons of the core that are only visible at low temperatures (Fig. S5), as observed during the reduction of pentacene.[19] Interestingly, the upshift is most pronounced for H_g (*ca.* 6.9 ppm) and H_f (*ca.* 5.7 ppm) protons and least pronounced for protons H_b (*ca.* 3.4 ppm). This is consistent with the additional electron density concentrated towards the center of the PPP core and ethynyl fragment and the tropicity of the rings. In contrast to the protons of the core,

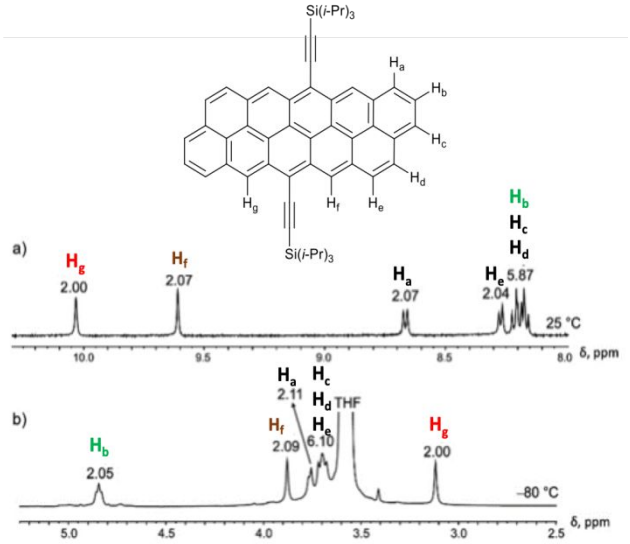

Fig. 6 ^{1}H NMR spectra of **TIPS-PPP** at 25 °C (a) and **TIPS-PPP**$^{2-}$ at −80 °C (b) in THF- d_8 with integration and peak assignment.

a minimal upfield shift is observed for the isopropyl protons of the side-group.

In summary, the first chemical reduction study of a vertically expanded functionalized pentacene and successful X-ray structural characterization of the doubly-reduced product have been accomplished. The use of sodium metal allowed the isolation of contact-ion complex in which the central edge of the polyaromatic core together with an acetylenic carbon provide the coordination site for the Na^+ ions. Bond length analysis shows that the dianion can be written with four aromatic sextets in agreement with the Clar representation. Although **TIPS-PPP**$^{2-}$ has 36 π-electrons (4n), it does not show a global or local magnetic paratropic response. On the contrary, on the whole, the dianion should be considered as a non-aromatic molecule.

Data Availability

The data that support the findings of this study are available in the ESI of this article. Crystallographic data have been deposited at the Cambridge Crystallographic Data Center as 2367428. These data can be obtained free of charge via htttps://www.ccdc.cam.ac.uk/data_request/cif.

Conflicts of interest

There are no conflicts to declare.

Acknowledgements

Dr. Zhe Wang is acknowledged for his help in the calculations of NICS. Financial support from NSF CHE-2404031 is gratefully acknowledged by M. A. P. NSF's ChemMatCARS, Sector 15 at the Advanced Photon Source (APS), Argonne National Laboratory (ANL) is supported by the Divisions of Chemistry (CHE) and Materials Research (DMR), National Science Foundation, under grant number NSF/CHE- 1834750. This research used resources of the Advanced Photon Source, a U.S. Department of Energy (DOE) Office of Science user facility operated for the DOE Office of Science by Argonne National Laboratory under Contract No. DE-AC02-06CH11357.

Notes and references

1 Q. Ye and C. Chi, *Chem. Mater.*, 2014, **26**, 4046–4056.
2 J. E. Anthony, *Angew. Chem. Int. Ed.*, 2008, **47**, 452–483.
3 S. A. Odom, S. R. Parkin and J. E. Anthony, *Org. Lett.*, 2003, **5**, 4245–4248.
4 Y.-F. Lim, Y. Shu, S. R. Parkin, J. E. Anthony and G. G. Malliaras, *J. Mater. Chem.*, 2009, **19**, 3049–3056.
5 F. Zhang, C. Melzer, A. Gassmann, H. von Seggern, T. Schwalm, C. Gawrisch and M. Rehahn, *Org. Electron.*, 2013, **14**, 888–896.
6 J. Zhang, R. H. Pawle, T. E. Haas and S. W. Thomas III, *Chem. – Eur. J.*, 2014, **20**, 5880–5884.
7 S. Kazim, F. J. Ramos, P. Gao, M. K. Nazeeruddin, M. Grätzel and S. Ahmad, *Energy Environ. Sci.*, 2015, **8**, 1816–1823.
8 P. Schäfer, L. Gartzia-Rivero, M.-T. Kao, C. Schäfer, S. Massip, C. de Vet, G. Raffy and A. D. Guerzo, *J. Mater. Chem. C*, 2021, **9**, 136–147.
9 E. B. Pereira, J. Bassaler, H. Laval, J. Holec, R. Monflier, F. Mesnilgrente, L. Salvagnac, E. Daran, B. Duployer, C. Tenailleau, A. Gourdon, A. Jancarik and I. Séguy, *RSC Adv.*, 2022, **12**, 671–680.
10 T. Zeng, R. Hoffmann and N. Ananth, *J. Am. Chem. Soc.*, 2014, **136**, 5755–5764.
11 S. M. Hart, W. Ruchira Silva and R. R. Frontiera, *Chem. Sci.*, 2018, **9**, 1242–1250.
12 D. Lubert-Perquel, E. Salvadori, M. Dyson, P. N. Stavrinou, R. Montis, H. Nagashima, Y. Kobori, S. Heutz and C. W. M. Kay, *Nat. Commun.*, 2018, **9**, 4222.
13 B. S. Basel, C. Hetzer, J. Zirzlmeier, D. Thiel, R. Guldi, F. Hampel, A. Kahnt, T. Clark, D. M. Guldi and R. R. Tykwinski, *Chem. Sci.*, 2019, **10**, 3854–3863.
14 K. J. Thorley and J. E. Anthony, *Isr. J. Chem.*, 2014, **54**, 642–649.
15 J. E. Anthony, J. S. Brooks, D. L. Eaton and S. R. Parkin, *J. Am. Chem. Soc.*, 2001, **123**, 9482–9483.
16 J. E. Anthony, D. L. Eaton and S. R. Parkin, *Org. Lett.*, 2002, **4**, 15–18.
17 T. Jousselin-Oba, M. Mamada, K. Wright, J. Marrot, C. Adachi, A. Yassar and M. Frigoli, *Angew. Chem. Int. Ed.*, 2022, **61**, e202112794.
18 S. Zhang, F. Talnack, T. Jousselin-Oba, V. Bhat, Y. Wu, Y. Lei, Y. Tomo, H. Gong, L. Michalek, D. Zhong, C. Wu, A. Yassar, S. Mannsfeld, C. Risko, M. Frigoli and Z. Bao, *J Mater. Chem. C*, 2023, **11**, 8992–9001.
19 M. Pennachio, Z. Zhou, Z. Wei, S. Liu, A. Yu. Rogachev and M. A. Petrukhina, *Chem. – Eur. J.*, 2022, **28**, e202104194.
20 R. Gershoni-Poranne and A. Stanger, *Chem. – Eur. J.*, 2014, **20**, 5673–5688.
21 Z. Zhou, X.-Y. Wang, Z. Wei, K. Müllen and M. A. Petrukhina, *Angew. Chem. Int. Ed.*, 2019, **58**, 14969–14973.
22 Z. Zhou, Z. Wei, Y. Tokimaru, S. Ito, K. Nozaki and M. A. Petrukhina, *Angew. Chem. Int. Ed.*, 2019, **58**, 12107–12111.
23 J. Kruszewski and T. M. Krygowski, *Tetrahedron Lett.*, 1972, **13**, 3839–3842.
24 Y. Gu, Y. G. Tullimilli, J. Feng, H. Phan, W. Zeng and J. Wu, *Chem. Commun.*, 2019, **55**, 5567–5570.
25 I. Rončević, F. J. Leslie, M. Rossmannek, I. Tavernelli, L. Gross and H. L. Anderson, *J. Am. Chem. Soc.*, 2023, **145**, 26962–26972.
26 E. Steiner and P. W. Fowler, *J. Phys. Chem. A*, 2001, **105**, 9553–9562.

Data Availability

The data that support the findings of this study are available in the ESI of this article. Crystallographic data have been deposited at the Cambridge Crystallographic Data Center as 2367428. These data can be obtained free of charge via htttps://www.ccdc.cam.ac.uk/data_request/cif.